Color Constancy Using Single Colors

Simone Bianco

University of Milano-Bicocca, Italy

Abstract. This work investigates if the von Kries adaptation can be generalized to deal with single colored patches. We investigate which colored patches can give statistically equivalent performance to a white patch for von Kries adaptation. The investigation is then extended to couples of colors, and the analysis of the characteristics of the colors forming the couples is carried out. We focus here on single and couples of colors since common objects and logos are usually composed by a small number of colors.

1 Introduction

Computational color constancy aims to estimate the actual color in an acquired scene disregarding its illuminant. Many illuminant estimation solutions have been proposed in the last few years [1,2], although it is known that the problem addressed is actually ill-posed as its solution lacks uniqueness and stability [3]. A recent research area which has shown promising results aims to improve illuminant estimation by using visual information automatically extracted from the images. The existing algorithms exploit both low-level [4,5], intermediate-level [6] and high-level [7] visual information.

In [7] several illuminant estimation approaches are applied to compute a set of possible illuminants. For each of them an illuminant color corrected image is evaluated on the likelihood of its semantic content: is the grass green, the road grey, and the sky blue, in correspondence with our prior knowledge of the world. The illuminant resulting in the most likely semantic composition of the image is selected as the illuminant color. In [8] an object-based approach is used for illuminant classification: only the pixel associated to an object are considered in the illuminant classification process using the object's spectral characteristics.

It has been shown that memory colors could be used as hints to give a more accurate estimate of the illuminant color in the scene. For example, Moreno et al. [9] obtained memory colors for three different objects (grass, snow and sky) using psychophysical experiments. A different approach has been used in [10] where a face detector was used to find faces in the scene, and the corresponding skin colors were used to estimate the chromaticity of the illuminant.

In this work we investigate if single colors can be used to estimate the illuminant color in the scene. We focus here on single colors since common objects (see Fig. 1.a which contains some examples extracted from the ALOI dataset [11]) and logos (see Fig. 1.b) are usually composed by a small number of colors. The idea is that if we are able to automatically recognize objects and logos that have

A. Fusiello et al. (Eds.): ECCV 2012 Ws/Demos, Part II, LNCS 7584, pp. 390–400, 2012.

a) b)

Fig. 1. a) Examples of common objects extracted from the ALOI dataset [11]; b) examples of common logos (http://www.flickr.com/photos/27845211@N02/2662264721/sizes/l/in/pool-75819424@N00/)

intrinsic colors, we could use them for color constancy. If the reflectance of the color and the sensor transmittance curves are known, it is possible to recover the illuminant power spectrum distribution in the set of a finite-dimensional linear model [12]. If the same color has been acquired under different illuminants, it is possible to classify the scene illuminant in one of the known illuminant classes [13]. We want here to relax these requirements: we assume to only know the sensor response of a reference colored patch under a canonical illuminant and under the scene illuminant. We investigate here for which colors the illuminant can be estimated as the ratio of the sensor response of the reference patch under the canonical illuminant and the sensor response of the same patch under the scene illuminant, giving statistically equivalent color constancy performance to those that would be obtained in the case of the classical von Kries white-patch normalization [14,15] (i.e. the reference patch is white). This investigation is then extended to couples of colors, analyzing the characteristics of the forming colors.

The procedure proposed can be applied to any colors, and is here illustrated for both the Gretag Macbeth ColorChecker DC chart and the Munsell atlas.

2 Problem Formulation and Proposed Solution

The image values for a Lambertian surface located at the pixel with coordinates (x, y) can be seen as a function $\boldsymbol{\rho}(x, y)$, mainly dependent on three physical factors: the illuminant spectral power distribution $I(\lambda)$, the surface spectral reflectance $S(\lambda)$ and the sensor spectral sensitivities $\mathbf{C}(\lambda)$. Using this notation $\boldsymbol{\rho}(x, y)$ can be expressed as

$$\boldsymbol{\rho}(x, y) = \int_{\omega} I(\lambda) S(x, y, \lambda) \mathbf{C}(\lambda) \mathrm{d}\lambda, \tag{1}$$

where ω is the wavelength range of the visible light spectrum, $\boldsymbol{\rho}$ and $\mathbf{C}(\lambda)$ are three-component vectors.

The aim of any color constancy algorithm [16] is to transform the color observation vector $\boldsymbol{\rho}$ to its corresponding illuminant-independent descriptor $\mathbf{d}$:

$$\mathbf{d} = \mathcal{Q}\boldsymbol{\rho}, \tag{2}$$

where $\mathcal{Q}$ is a linear transform. Following [16], we constrain $\mathcal{Q}$ to be diagonal. In this work the Forsyth's definition of descriptor is used [17], which is defined as the observation of a surface seen under a canonical illuminant.

$$\mathbf{d}_i^c \equiv \boldsymbol{\rho}_i^c = \int_\omega I_c(\lambda) S_i(\lambda) \mathbf{C}(\lambda) \mathrm{d}\lambda, \tag{3}$$

In the von Kries adaptation [14], or white-patch normalization, the descriptor for a surface i acquired under an unknown illuminant e is obtained as follows:

$$\mathbf{d}_i^e = \mathcal{D}^{e,c} \boldsymbol{\rho}_i^e \tag{4}$$

with

$$\mathcal{D}^{e,c} = \left[\mathrm{diag}\left(\boldsymbol{\rho}_w^e\right)\right]^{-1} \tag{5}$$

where $\boldsymbol{\rho}_w^e$ corresponds to the image values of a white surface acquired under the unknown illuminant.

Since a white surface is not always available in the acquired scene, in this work we want to see if other colors can be used to obtain the illuminant compensation matrix $\mathcal{D}^{e,c}$. This would enable to use colored objects (eventually automatically detected in the scene), to be used to derive the diagonal mapping $\mathcal{D}^{e,c}$ given only their representation under a canonical illuminant c, without further knowledge of both the object spectral reflectance and the camera sensor transmittances.

Given only $\boldsymbol{\rho}_i^e$ and its acquired values under a canonical illuminant $\boldsymbol{\rho}_i^c$, $\mathcal{D}^{e,c}$ can be obtained as

$$\mathcal{D}^{e,c} = \frac{\mathrm{diag}\left(\boldsymbol{\rho}_i^c / \boldsymbol{\rho}_i^e\right)}{|| \left(\boldsymbol{\rho}_i^c / \boldsymbol{\rho}_i^e\right) ||_\infty} \tag{6}$$

which for the case of a white surface corresponds to the white-patch normalization [14,15].

The estimation described in Eq. 6 can be extended to two or more colors in different ways [13,17]. In this work we consider the easiest extension: given n corresponding colors seen under the canonical and the scene illuminant, the diagonal mapping is estimated as the average of the single estimations given by each color taken individually, i.e.

$$\mathcal{D}^{e,c} = \frac{1}{n} \sum_{i=1}^{n} \frac{\mathrm{diag}\left(\boldsymbol{\rho}_i^c / \boldsymbol{\rho}_i^e\right)}{|| \left(\boldsymbol{\rho}_i^c / \boldsymbol{\rho}_i^e\right) ||_\infty} \tag{7}$$

Furthermore, the estimation described in Eq. 5 can be extended to the case of generalized diagonal transforms which are able convey higher color constancy performance [16]. Let $\mathcal{T}$ be the sensor sharpening transformation, than Eq. 5 becomes

$$\mathcal{D}^{e,c} = \mathcal{T}^{-1} \left[\mathrm{diag}\left(\mathcal{T} \boldsymbol{\rho}_w^e\right)\right]^{-1} \mathcal{T} \tag{8}$$

The extensions of Eq.6 and 7 for the case of generalized diagonal transforms are straightforward.

Given a set of colors $i = 1, \ldots, m$, we want to find those which can be used to estimate a diagonal mapping $\mathcal{D}^{e,c}$ with statistically equivalent color constancy performance to those that would be obtained using a white surface. The color constancy performance are measured for each color of the set using the normalized distance (ND) metric [16], which is defined as

$$\text{ND} = 100 * \frac{||\mathbf{d}_i^e - \mathbf{d}_i^c||}{||\mathbf{d}_i^c||} \tag{9}$$

where $\mathbf{d}_i^c$ denotes the canonical descriptor and $\mathbf{d}_i^e$ denotes the descriptor for the scene illuminant e. The cumulative ND histograms are calculated on all the color set, using each of the colors at turn to estimate the diagonal mapping $\mathcal{D}^{e,c}$, resulting in a total of m cumulative histograms. In order to determine if there are colors that can be used to obtain color constancy performance statistically equivalent to what can be obtained using a perfect white patch (i.e. perfectly spectrally flat reflectance spectrum), the Wilcoxon Signed-Rank Test [18] is used: a color is considered equivalent to an ideally white surface for von Kries adaptation, if the respective ND cumulative histograms are considered statistically equivalent by the Wilcoxon test.

3 Experimental Results

The experimental results are obtained with simulated data using the theoretical model of image formation reported in Eq. 1. For the sensor spectral sensitivities $\mathbf{C}(\lambda)$, 7 different filter sets are used: 6 correspond to measured sensor sensitivities of digital cameras (i.e. Nikon D1, Nikon D70, Nikon D100, Nikon D5000, Canon 500D, and Sony DXC930); the remaining one are the XYZ color matching functions. The illuminant spectral power distributions are the same 14 used in [19], i.e.: six CIE daylight illuminants (D48, D55, D65, D75, D100, D200), three CIE standard illuminants (A, B, C), a 2000 K Planckian blackbody radiator, a uniform white (UW), and three fluorescent illuminants (F2, F7, F11). The surface spectral reflectances are those of the Gretag Macbeth ColorChecker DC chart (MDC), which is composed of 180 different colored patches.

The color constancy performance are measured using the normalized distance (ND) metric (see Eq.9), choosing the white-patch descriptor vectors calculated for D65 as the canonical descriptor vectors. We consider a color equivalent to an ideally white surface for von Kries adaptation, if the respective ND cumulative histograms are considered statistically equivalent by the Wilcoxon test under all the 14 illuminants considered. As an example, the ND cumulative histrograms under all the 14 illuminants using the XYZ color matching functions are reported in Fig. 2. Each line corresponds to a different color of the MDC. The red lines correspond to the colored patches considered statistically equivalent to an ideally white surface for von Kries adaptation.

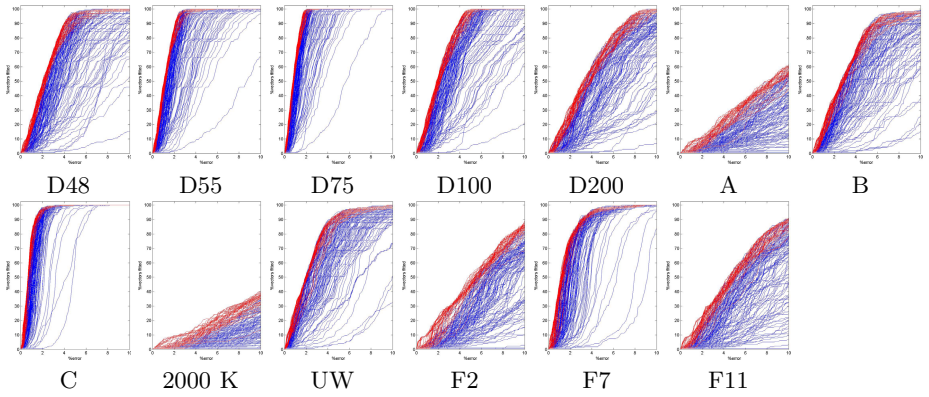

Fig. 2. ND cumulative histrograms under all the 14 illuminants using the XYZ color matching functions. The red lines correspond to the colored patches considered statistically equivalent to an ideally white surface for von Kries adaptation.

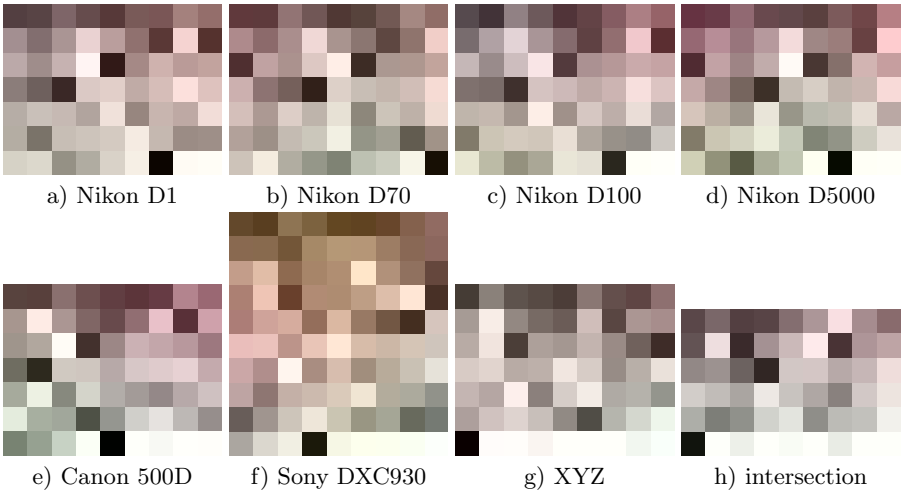

Fig. 3. Patches of the MDC chart considered statistically equivalent to an ideally white surface for von Kries adaptation under all the 14 illuminants for each of the sensor filter sets considered (a-g); intersection of all the patches extracted (h)

In Fig. 3 the patches of the MDC chart considered statistically equivalent to an ideally white surface for von Kries adaptation under all the 14 illuminants are reported for each of the sensor filter sets considered. The intersection of all the patches extracted are also reported.

In Fig. 4 the patches of the MDC chart are plotted in the CIEL*a*b* color space. They are plotted distinguishing the patches considered statistically equivalent to an ideally white surface (black crosses) from those which are not (red dots).

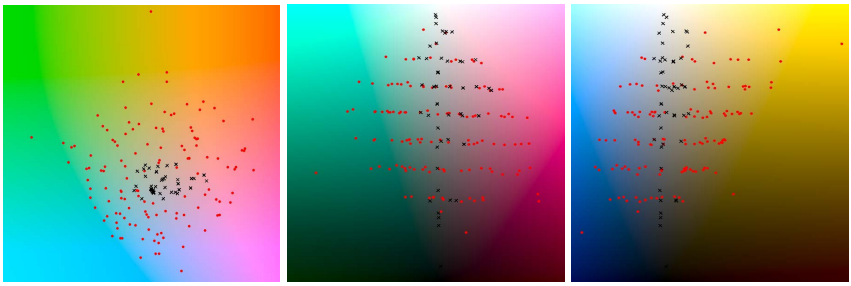

a) b) c)

Fig. 4. Patches of the MDC chart reported in the CIEL*a*b* color space: a*b* plane (a), a*L* plane (b), b*L* plane (c). Black crosses: patches considered statistically equivalent to an ideally white surface; red dots: the remaining patches.

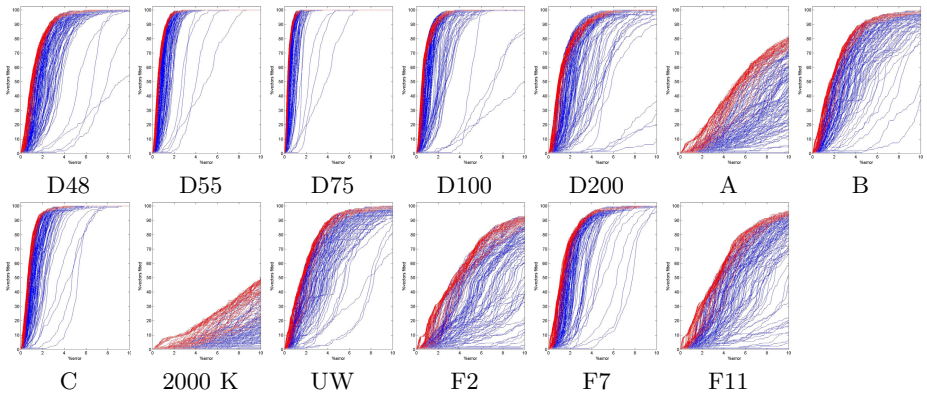

Fig. 5. ND cumulative histrograms under all the 14 illuminants using the XYZ color matching functions with the CAT02 chromatic adaptation transform. The red lines correspond to the colored patches considered statistically equivalent to an ideally white surface for von Kries adaptation.

Since it is known that generalized diagonal transforms are able to convey higher color constancy performance [16], we investigate how the use of the CAT02 chromatic adaptation transform [20] modifies the ND cumulative histograms (Fig. 5) and the extracted patches (Fig.6.a) when the XYZ color matching functions are used. In order to have a more compact representation of which hues are most present among the extracted patches, we also plot their color names histogram [21] where to each patch the name with the highest probability is assigned (Fig.6.b); the 11 color names considered are the same used in [21], i.e.: black, blue, brown, gray, green, orange, pink, purple, red, white, and yellow. In the case of sensor transmittances different from the XYZ, it is still possible to compute a sharpening transform using for example the method described in [22].

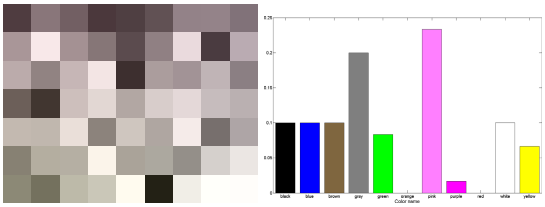

a) b)

Fig. 6. Patches of the MDC chart considered statistically equivalent to an ideally white surface for von Kries adaptation under all the 14 illuminants using the XYZ color matching functions with the CAT02 chromatic adaptation transform (a). Their color names histogram (b).

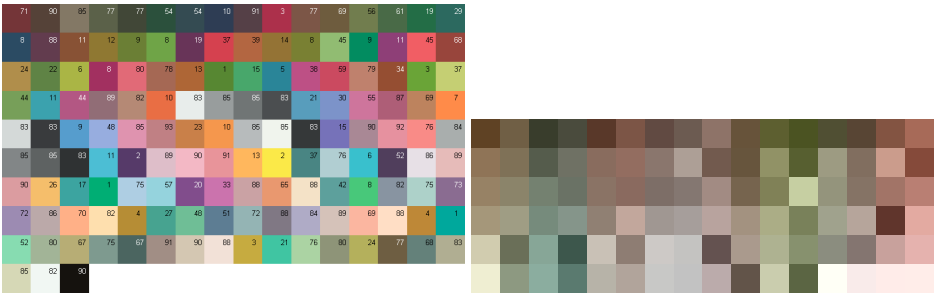

a) b)

Fig. 7. Patches composing the couples that considered statistically equivalent to a white patch (a). Remaining patches after removing all the couples containing one of the patches reported in Fig. 3.h.

From the comparison of Fig. 5 and Fig. 2 it is possible to notice how all the ND cumulative histograms have been moved towards the upper left corner of the plot, indicating higher color constancy performance under all the illuminants considered. Together with the increase in color constancy performance, the use of the chromatic adaptation transform is also able to increase the number of colored patches considered statistically equivalent to an ideally white surface for von Kries adaptation: using the CAT02 the number of extracted patches is 60, while using only the XYZ CMF it was 55, which is almost a 9.1% increase.

The analysis on single colors is now extended to couples of colors using Eq. 7 for the computation of the diagonal mapping. In Fig. 7 the patches that compose the couples considered statistically equivalent to an ideally white surface for von Kries adaptation under all the 14 illuminants with all the filter sets considered are reported. In the upper right corner of each colored patch is reported the number of extracted couples in which it appeared.

In Fig. 8 the patches of the MDC chart are plotted in the CIEL*a*b* color space. They are plotted distinguishing the patches which formed couples

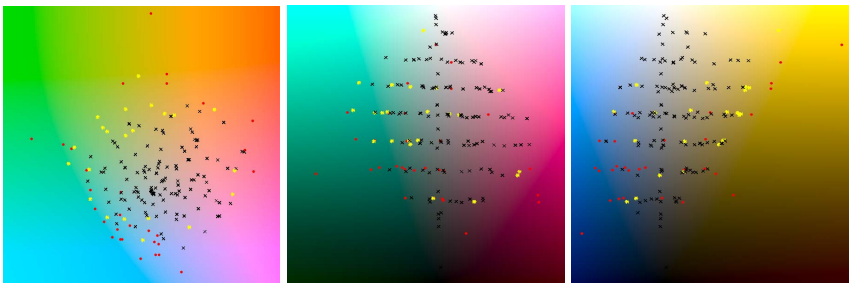

a) b) c)

Fig. 8. Patches of the MDC chart reported in the CIEL*a*b* color space: a*b* plane (a), a*L* plane (b), b*L* plane (c). Black crosses: patches in couples considered statistically equivalent to an ideally white surface and appeared in more than 10 couples; yellow stars: patches appeared in less than 10 couples; red dots: the remaining patches.

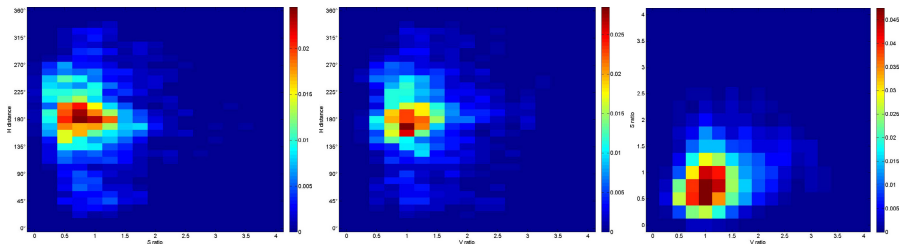

a) b) c)

Fig. 9. 2D histograms of the angular distance between the hues, the ratio of the saturations, and the ratio of the values for the colors forming the couples.

considered statistically equivalent to an ideally white surface and appeared in more than 10 couples (black crosses), from those in couples statistically equivalent but appeared in less than 10 couples (yellow stars), from those in couples not statistically equivalent (red dots).

In order to investigate how the couples are composed, we first eliminate all the couples in which at least one of the colors is one of those reported in Fig. 3.h. The remaining colors are reported in Fig. 7.b. The couples formed by the colors in Fig. 7.b are then analyzed as follows: the two colors are converted into the HSV color space and then the angular distance between the hues, the ratio of the saturations, and the ratio of the values are computed. The 2D histograms of these 3 quantities are reported in Fig. 9.

From the histograms reported in Fig. 9 it is possible to see that the couples are mostly composed of opponent colors (the H distance is mainly included in the $[135°, 270°]$ interval); it is also possible to note that there is a number of couples that satisfy the gray world assumption [23] (i.e. their average color is gray): they correspond to the bin in the histogram with H distance equal to 180° and S ratio equal to 1.

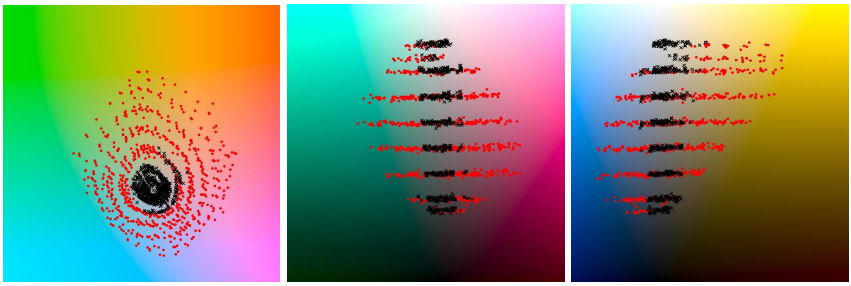

Fig. 10. Patches of the Munsell atlas reported in the CIEL*a*b* color space: a*b* plane (a), a*L* plane (b), b*L* plane (c). Black crosses: patches considered statistically equivalent to an ideally white surface; red dots: the remaining patches.

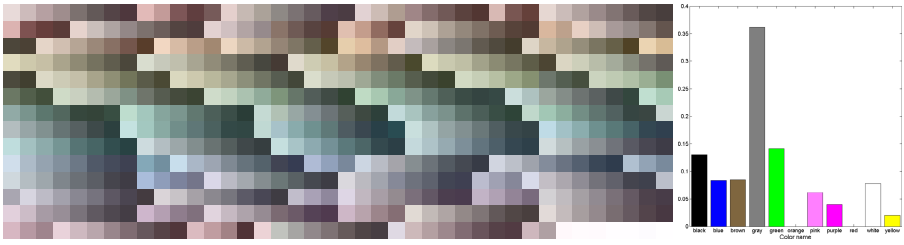

a) b)

Fig. 11. Patches of the Munsell atlas considered statistically equivalent to an ideally white surface for von Kries adaptation under all the illuminants and sensor filter sets considered (a). Their color names histogram (b).

In order to have a more populated plots than those reported in Fig. 4, the same analysis carried out for the MDC chart, is now applied to the Munsell atlas. The single colors considered statistically equivalent to an ideally white surface for von Kries adaptation are reported in Fig. 10 and 11.a. In Fig.11.b their color names [21] histogram are also reported, where to each patch the name with the highest probability is assigned.

4 Conclusions

In this work it has been investigated if the von Kries adaptation can be generalized to colored patches. In fact von Kries adaptation is a channel-independent scaling where each component is the reciprocal of the sensor response induced from a reference patch, which is usually white. This paper gives a procedure to determine which colored patches can give statistically equivalent performance to a white patch for von Kries adaptation. The simulations have been carried

out 14 different illuminants and 7 different sensor sets. The investigation is then extended to couples of colors, and the analysis of the characteristics of the colors forming the extracted couples is carried out. The procedure can be applied to color sets of any cardinality; the results can not be given here due to the lack of space.

References

1. Hordley, S.D.: Scene illuminant estimation: past, present, and future. Color Research & Application 31(4), 303–314 (2006)
2. Gijsenij, A., Gevers, T., van de Weijer, J.: Computational color constancy: survey and experiments. IEEE TIP 20(9), 2475–2489 (2011)
3. Funt, B., Barnard, K., Martin, L.: Is Machine Colour Constancy Good Enough? In: Burkhardt, H.-J., Neumann, B. (eds.) ECCV 1998. LNCS, vol. 1406, pp. 445–459. Springer, Heidelberg (1998)
4. Bianco, S., Ciocca, G., Cusano, C., Schettini, R.: Automatic Color Constancy Algorithm Selection and Combination. Pattern Recognition 43(3), 695–705 (2010)
5. Gijsenij, A., Gevers, T.: Color Constancy using Natural Image Statistics and Scene Semantics. IEEE TPAMI 33(4), 687–698 (2011)
6. Bianco, S., Ciocca, G., Cusano, C., Schettini, R.: Improving Color Constancy Using Indoor-Outdoor Image Classification. IEEE TIP 17(12), 2381–2392 (2008)
7. van de Weijer, J., Schmid, C., Verbeek, J.: Using High-Level Visual Information for Color Constancy. In: IEEE ICCV, pp. 1–8 (2007)
8. Hel-Or, H.Z., Wandell, B.A.: Object-based illuminant classification. Pattern Recognition 35(8), 1723–1732 (2002)
9. Moreno, A., Fernando, B., Kani, B., Saha, S., Karaoglu, S.: Color Correction: A Novel Weighted Von Kries Model Based on Memory Colors. In: Schettini, R., Tominaga, S., Trémeau, A. (eds.) CCIW 2011. LNCS, vol. 6626, pp. 165–175. Springer, Heidelberg (2011)
10. Bianco, S., Schettini, R.: Color constancy using faces. In: IEEE CVPR, pp. 65–72 (2012)
11. Geusebroek, J.M., Burghouts, G.J., Smeulders, A.W.M.: The Amsterdam library of object images. IJCV 61(1), 103–112 (2005)
12. Wandell, B.A.: The synthesis and analysis of color images. IEEE TPAMI 9(1), 2–13 (1987)
13. Finlayson, G.D., Hordley, S.D., Hubel, P.M.: Color by correlation: a simple, unifying framework for color constancy. IEEE TPAMI 23(11), 1209–1221 (2001)
14. West, G., Brill, M.H.: Necessary and sufficient conditions for von Kries chromatic adaptation to give colour constancy. J. of Math. Biol. 15, 249–258 (1982)
15. Land, E.H.: The retinex theory of color vision. Scientific American 237(6), 108–128 (1977)
16. Finlayson, G.D., Drew, M.S., Funt, B.V.: Color constancy: generalized diagonal transforms suffice. JOSA A 11(11), 3011–3019 (1994)
17. Forsyth, D.: A novel algorithm for color constancy. IJCV 5, 5–36 (1990)
18. Wilcoxon, F.: Individual comparisons by ranking methods. Biometrics 1, 80–83 (1945)
19. Bianco, S., Bruna, A., Naccari, F., Schettini, R.: Color space transformations for digital photography exploiting information about the illuminant estimation process. JOSA A 29(3), 374–384 (2012)

20. Moroney, N., Fairchild, M.D., Hunt, R.W.G., Li, C., Luo, M.R., Newman, T.: The CIECAM02 Color Appearance Model. In: Proc. of the 10th CIC, pp. 23–27 (2002)
21. van de Weijer, J., Schmid, C., Verbeek, J., Larlus, D.: Learning Color Names for Real-World Applications. IEEE TIP 18(7), 1512–1524 (2009)
22. Chong, H.Y., Gortler, S.J., Zickler, T.: The von Kries hypothesis and a basis for color constancy. In: IEEE ICCV, pp. 1–8 (2007)
23. Buchsbaum, G.: A spatial processor model for object color perception. Journal of Franklin Institute 310, 1–26 (1980)